JOURNAL OF SOLID STATE CHEMISTRY 103, 504–513 (1993)

Electrical Properties and Phase Transitions in Superconducting Quasi-One-Dimensional Chalcogenides $In_xNb_3X_4$ (X = S, Se, and Te)

T. OHTANI,* Y. SANO, AND Y. YOKOTA†

Laboratory for Solid State Chemistry and †Research Center for Microanalysis, Okayama University of Science, Ridai-cho 1-1, Okayama 700, Japan

Received May 11, 1992; in revised form September 24, 1992; accepted September 28, 1992

Electrical properties and phase transitions were investigated in the quasi-one-dimensional ternary chalcogenides $In_xNb_3X_4$ (X = S, Se, and Te; x = 0.5 for X = S, and 1.0 for X = Se and Te), with results indicating that the $In_xNb_3Te_4$ system has two new kinds of phase transitions. Based on the values of the transition temperatures T_t, this system is classified into two groups, i.e., Group 1 samples with $0 \le x < 0.55$ having T_t = ≈40 and ≈80 K, and Group 2 samples with $0.55 < x \le 1.0$ having T_t = ≈50 and ≈140 K. Electron diffraction measurements showed the 140-K transition to be associated with a charge-density-wave (CDW) formation accompanied by the appearance of a superstructure that can be explained by the commensurate wave vectors $q = \pm(\frac{1}{4}a^* + \frac{1}{3}b^*) + \frac{2}{3}c^*$, which are slightly larger in the c^* component as compared with those previously observed in Nb_3Te_4 of $q = \pm(\frac{1}{4}a^* + \frac{1}{3}b^*) + \frac{2}{3}c^*$. The increase in the c^* component was interpreted as being caused by the increase in Fermi energy due to In insertion. Thermopower measurements on $In_xNb_3Te_4$ showed the dominant carriers to be holes. In addition, the $In_xNb_3Se_{3.84}$ system ($0.40 \le x \le 1.0$) showed a new CDW-like transition at ≈30 K. The superconducting critical temperature T_c of $In_xNb_3X_4$ was increased by several degrees when the In content x was increased above 0.5. © 1993 Academic Press, Inc.

Introduction

Many transition metal chalcogenides have low-dimensional structures due to the inherent large covalency of their metal–chalcogen bonds. Following the discovery of charge-density-wave (CDW) instabilities in many layered transition metal chalcogenides (*1*), numerous low-dimensional chalcogenides displaying CDW transitions have been found, with subsequent research interest in the 1980s being mainly focused on CDW transport, i.e., the nonlinear conduction resulting from the sliding of CDWs (*2*).

Figure 1 shows the crystal structure of Nb_3X_4 (X = S, Se, and Te). The compounds have a hexagonal cell (space group $P6_3$), which is built up by NbS_6 octahedra linked together via shared faces and edges (*3*, *4*). This structure is characterized by zigzag Nb–Nb chains running parallel to the c axis, and also by large hexagonal tunnels running along the same direction. The Nb chains are depicted in Fig. 1 by the neighboring Nb atoms that are shown linked together. Since the Nb–Nb distance along the chains is close to that in pure Nb metal, as well as the Nb chains being well separated from

* To whom correspondence should be addressed.

0022-4596/93 $5.00

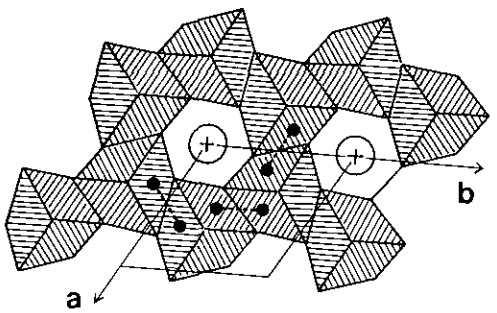

FIG. 1. Crystal structure of Nb_3X_4 (X = S, Se, and Te) (hexagonal; space group $P6_3$) looking down the c axis. The structure is built up by NbX_6 octahedra, which are linked by shared faces and edges. Nb–Nb zigzag chains are running parallel to the c axis. The chains are depicted by two neighboring closed circles linked together by the dashed lines; for simplicity only three chains are shown. Large hexagonal tunnels also run along the c axis, being able to accommodate the ternary elements (ions) as shown by the large open circles together with the plus mark.

one another by the chalcogen atoms, these compounds can be considered as having quasi-one-dimensional structures.

Many ternary isotypic compounds have been found, i.e., TlV_6S_8 (*5, 6*), $TlTi_6Se_8$ (*7*), KTi_6Se_8 and AV_6X_8 (A = K, Rb, and In; X = S, Se, and Te) (*8*), $K_{0.2}V_6S_8$ (*9*), ANb_6X_8 (A = alkali metals, Ag, Zn, Pb, In, Tl, etc.; X = S, Se, and Te) (*7, 10–12*).

Amberger *et al.* found superconductivity in Nb_3X_4 for X = S, Se, and Te having respective critical temperatures T_c = 4.0, 2.0, and 1.8 K (*13*). Detailed electrical properties of Nb_3X_4 were subsequently reported by Ishihara and Nakada who observed highly anisotropic resistivity ρ (*14*) and in both Nb_3S_4 and Nb_3Se_4 a T^3 dependence of ρ along the c axis in the low temperature region (*14, 15*). Theoretical electronic structures of Nb_3X_4 were presented by Oshiyama (*16, 17*) and Bullett (*18*) on the basis of the linear combinations of atomic orbitals (LCAO) method, and by Canadell and Whangbo (*19*) who performed a tight-binding calculation. The resultant band structures calculated by these studies correlate well, thereby clearly indicating a pseudo-one-dimensional nature. Oshiyama (*16, 17*) reported that the Fermi surfaces consist of three warped undulating plane sheets perpendicular to the c axis, which correspond with the three Nb zigzag chains within a unit cell, and furthermore showed that the T^3 dependence of ρ can be explained by electron–electron Umklapp scattering processes associated with the calculated Fermi surfaces (*16, 17*).

Ishihara and Nakada also observed two types of phase transitions in Nb_3Te_4 at 38 and 80 K (*20, 21*), with Suzuki *et al.* (*22*) using electron diffraction (ED) measurements to show that the 80-K transition is associated with CDW formation. The superlattice spots they observed below 80 K were explained by commensurate wave vectors $q = \frac{2}{3}a^* \pm \frac{3}{7}c^*$. Contrastingly, Sekine *et al.* (*23*) used X-ray diffraction measurements to show that the superstructure of Nb_3Te_4 is characterized by commensurate wave vectors $q = \pm(\frac{1}{3}a^* + \frac{1}{3}b^*) + \frac{3}{7}c^*$, and suggested that the ED patterns reported by Suzuki *et al.* (*22*) should be analyzed with their newly found q vectors. It is generally known that the CDW state can coexist with the superconductivity state when the CDWs are weakened either by high pressure or through doping by impurities, e.g., as observed in $NbSe_3$ (*24, 25*). Nb_3Te_4, however, shows the ability to coexist under no special conditions; hence this compound is considered an excellent material for investigating why these conflicting phenomena coexist.

The tunnels in Nb_3X_4 are able to accommodate a large variety of ternary elements, thus leading to the chalcogenides of $A_xNb_3S_4$ (A = Li, Na, K, and Ca) being first prepared by Schöllhorn and Schramm (*10*) using primarily an electrochemical method. $Tl_xNb_3Se_4$ was prepared by Boller and Klepp (*7*), whereas Huan and Greenblatt prepared many other isotypic compounds: $A_xNb_3Se_4$ (A = Na, K, Rb, Cu, Ag, Zn, and Pb) (*11*) and $A_xNb_3X_4$ (A = Na, K, Rb, Cs,

Cu, Ag, In, Zn, Cd, Sn, Pb, and Bi for X = S and Te; A = Sn, Pb, and Bi (for X = Se) (*12*) by applying molten salt exchange or ternary element insertion methods. The insertion of ternary elements is generally expected to have significant effects on the physical properties of the host binary compounds (*19*), with Schöllhorn and Schramm (*10*) reporting that the superconducting critical temperature T_c of Nb_3S_4 is increased by the introduction of potassium, i.e., T_c = 7.3 K for $K_{0.2}Nb_3S_4$. Huan and Greenblatt (*12*) reported that T_c values for the ternary phases of $Pb_{0.5}Nb_3Se_4$, $InNb_3Te_4$, and $Zn_{0.5}Nb_3Te_4$ are considerably higher than that of the corresponding binary phases. However, more detailed T_c studies, as well as other physical properties in these ternary chalcogenides, have not yet been reported.

In the present study, electrical measurements (electrical resistivity and thermopower: Seebeck coefficients) were carried out on $In_xNb_3X_4$ (X = S, Se, and Te) in order to investigate both the phase transitions and the superconductivity. In addition, electron diffraction studies were performed on $In_xNb_3Te_4$ to elucidate existing transition mechanisms.

Experimental

Specimens of $In_xNb_3X_{4-y}$ (X = S, Se and Te; $0 \leq x \leq 1.0$) were prepared by heating mixtures of the desired ratio of In metal and Nb_3X_{4-y} in evacuated silica tubes at 400°C for 1 week, where Nb_3X_{4-y} was first prepared by heating the appropriate mixture of elements in silica tubes at 1100°C for 2 weeks. Obtained specimens were pelletized under a 2000-kg/cm^2 pressure, sintered for 1 week in silica tubes at 1000°C, and then annealed at 400°C for 1 week in order to eliminate possible lattice defects. $In_xNb_3Se_{4-y}$ specimens were also obtained by heating a mixture of the desired ratio of elements at 1000°C for 1 week, and then annealed at 400°C after pelletizing. Nb_3X_4 single crystals were prepared by a chemical transport reaction using iodine as a transport agent. The transport tube had a 150-mm length, a 15-mm diameter, and a temperature gradient of 900–1000°C. The initial material was situated at the lower temperature side and the reaction duration was 1 week. Single crystals of Nb_3Te_4 were occasionally formed by the reaction of the elements without the use of the chemical transport technique. All the Nb_3X_4 single crystals had a bundled needle shape and were 5–10 mm in length. Suitable conditions to produce single crystals of $In_xNb_3X_4$ were not found. Chemical compositions of all the specimens were analyzed by an electron probe microanalyzer (X-650, Hitachi Co. and EMAX-2200, Horiba Co.), as well as by performing X-ray diffraction measurements (RAD-B, Rigaku Denki Co.).

Electrical resistivity was measured from 1.5 to 273 K by the conventional dc four probe method. The Seebeck coefficient S was measured for $In_xNb_3Te_4$ using a temperature gradient of 0.3 K/cm from 90 to 273 K using a similar method to that previously described (*26*). Temperature was measured with Au + 0.07 at% Fe vs Chromel thermocouples in both the electrical resistivity and thermopower measurements.

Electron diffraction measurements were performed using an electron microscope (JEM-4000EX and JEM-2000EX) down to ≈60 K for $In_xNb_3Te_4$ samples having various x values.

Results and Discussion

Resultant X-ray diffraction and EPMA data showed that the chalcogen content $(4 - y)$ in Nb_3X_{4-y} is at the most 3.84, 3.84, and 4.0 for X = S, Se, and Te, respectively, whereas for In, the maximum x content of $In_xNb_3X_{4-y}$ is 1.0 for X = Se and Te. However, for X = S, the x content is 0.5, a difference which is believed to indicate that Nb_3S_4 is less capable to accommodate the In atoms as compared with both Nb_3Se_4 and Nb_3Te_4

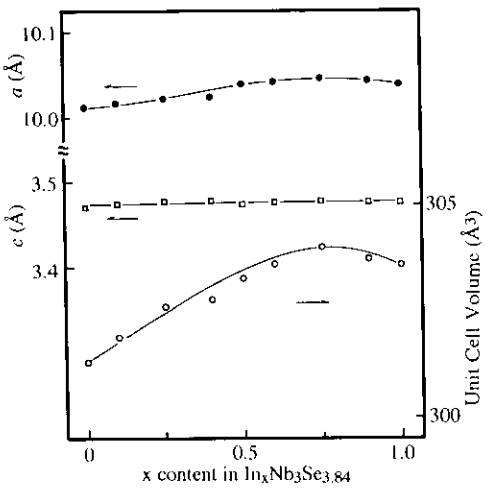

FIG. 2. Unit cell parameters of $In_xNb_3Se_{3.84}$ as a function of In content x.

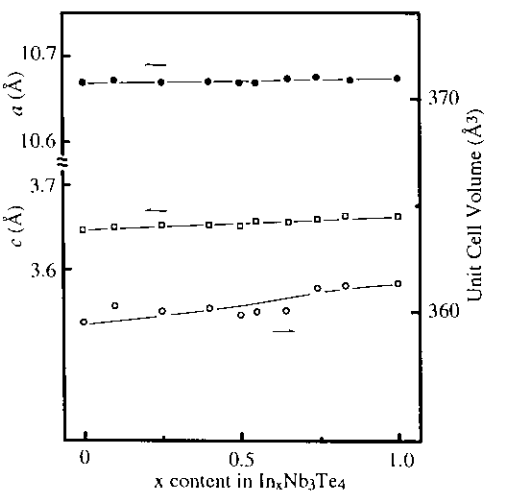

FIG. 3. Unit cell parameters of $In_xNb_3Te_4$ as a function of In content x.

which have larger tunnel sizes. In contrast to our results, Huan and Greenblatt (*11, 12*) previously prepared the compounds of $In_{0.5}Nb_3Se_4$, $In_{1.0}Nb_3Te_4$, and $In_{1.0}Nb_3S_4$. The reason for the discrepancy in In contents between the present and their samples is not clear, although the slight difference in the chalcogen contents may be most responsible for it.

Figure 2 shows cell parameters of $In_xNb_3Se_{3.84}$ ($0 \leq x \leq 1.0$) as a function of In content x, where the a vs x curve is concave downward and has a broad maximum around $x = 0.75$. On the other hand, c is almost constant with respect to x, probably due to that the tunnels are running along the c axis. Consequently, the cell volume also has a maximum near $x = 0.75$, with this anomaly around $x = 0.75$ therefore suggesting the existence of a new crystalline phase near this x content. In Fig. 3 the same parameters are shown for $In_xNb_3Te_4$ ($0 \leq x \leq 1.0$). The insertion of In atoms into Nb_3Te_4 obviously has less influence on the lattice parameters as compared with Nb_3Se_4, which is probably due to that the tunnel size in Nb_3Te_4 is larger than in Nb_3Se_4. For $In_xNb_3S_{3.84}$ samples with $x = 0$, 0.25, and 0.50, slight increases in both a and c were found as x increased.

Figure 4 shows the temperature variations of resistivity ρ along the c direction for single crystals of Nb_3X_4 (X = S, Se, and Te) from 4.2 to 273 K. Nb_3S_4 and Nb_3Se_4 show metallic behavior over the entire temperature range, whereas Nb_3Te_4 shows distinct ρ anomalies at ≈40 and ≈80 K, results similar to those observed by Ishihara and Nakada (*14, 15, 20, 21*).

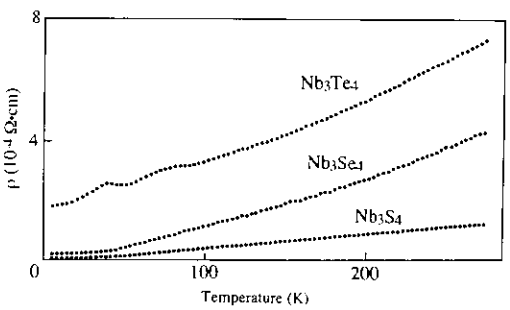

FIG. 4. Temperature variations of electrical resistivity ρ of single crystals of Nb_3X_4 (X = S, Se, and Te) along the c direction.

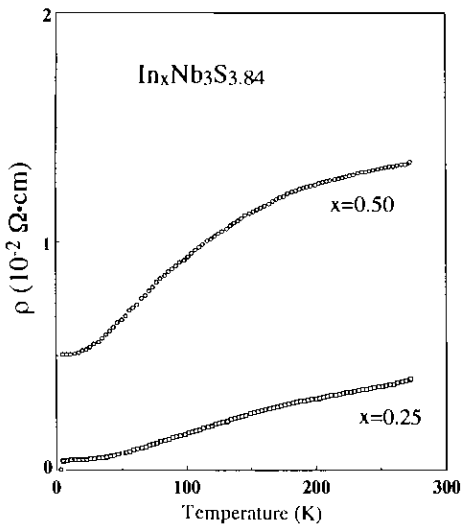

FIG. 5. Temperature variations of electrical resistivity ρ of polycrystalline $In_xNb_3S_{3.84}$ (x = 0.25 and 0.50).

The temperature variations of ρ for polycrystalline $In_xNb_3S_{3.84}$ with $x = 0.25$ and 0.50 are shown in Fig. 5 from 1.5 to 273 K, where both contents show metallic behavior. The cooling and heating results were consistent with each other. The increase in resistivity with increasing x is probably due to elongation of the Nb–Nb distance associated with lattice expansion caused by In insertion. Superconductivity was observed at 2.1 K for $x = 0.5$ as shown. It should be noted that the resistivity characteristics of both samples show a T^2 dependence rather than a T^3 one as previously reported (*14, 15*).

Figure 6 shows temperature variations of ρ for polycrystalline $In_xNb_3Se_{3.84}$ with x = 0.10, 0.25, 0.40, 0.75, and 1.0. Since the results were quite reversible in cooling and heating runs, only the cooling data are shown. The samples with $x \geq 0.40$ showed superconductivity at 2–3 K, although these data are not shown for the sake of simplicity. The noticeable result is that the resistivity shows a large jump at 25–45 K for the samples with $x \geq 0.40$. This jump in resistivity clearly indicates the existence of a new kind of phase transition which has not been reported in binary Nb_3Se_{4-y}. The most likely origin for this transition is the formation of a CDW, which is possibly supported by the sharp increase in ρ. Superlattice spots in the ED patterns could not be observed below the transition, probably due to heating effects caused by electron beam irradiation. The transition has the following interesting features: (1) The transition temperature is nearly constant with variations in In content x, and (2) The magnitude of the jump in ρ is most prominent in the $x = 0.75$ sample, with this composition corresponding to the maximum value of both a and the unit cell volume (Fig. 2). These results suggest the formation of a new kind of crystalline phase near $x = 0.75$ in the normal state above the phase transition, which may be related to the ordering of the inserted In atoms in $In_{0.75}Nb_3Se_{3.84}$. In preliminary ED studies carried out at room temperature, rather complex superlattice patterns were observed in this compound with $x = 0.75$; how-

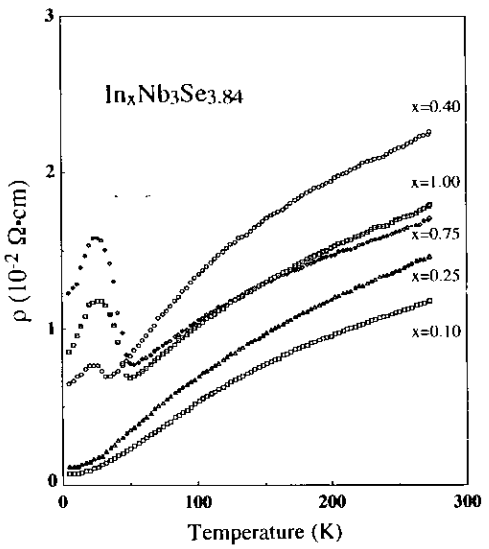

FIG. 6. Temperature variations of electrical resistivity ρ of polycrystalline $In_xNb_3Se_{3.84}$ (x = 0.10, 0.25, 0.40, 0.75, and 1.0).

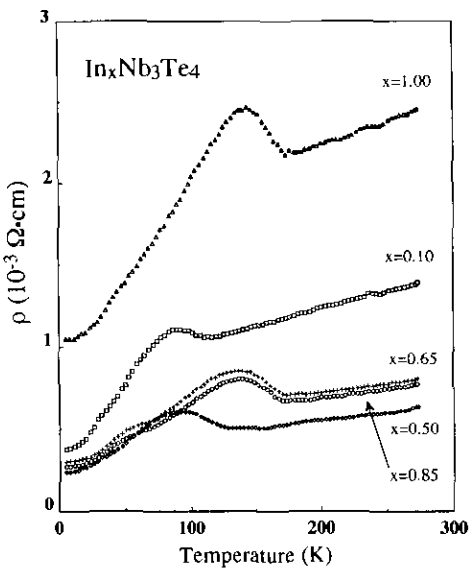

FIG. 7. Temperature variations of electrical resistivity ρ of polycrystalline $In_xNb_3Te_4$ (x = 0.10, 0.50, 0.65, 0.85, and 1.0).

ever, further research is necessary to obtain more detailed information on the crystalline structure.

Figure 7 shows temperature variations of ρ for polycrystalline $In_xNb_3Te_4$ with x = 0.10, 0.50, 0.65, 0.85, and 1.0. Only data from cooling experiments are shown, similarly to Fig. 6. Superconductivity was observed in samples with $x \geq 0.65$, although not shown to prevent confusion. Each sample shows two types of phase transitions, with no hysteresis being observed in any sample at either transition. The transition temperatures T_t are shown in Fig. 8 as a function of x, where the top and the bottom of the vertical bars respectively correspond to the onset and the maximum ρ value of the anomaly shown in Fig. 7. Based on the T_t values, this series of compounds is classified into two groups, i.e., Group 1 with $0 \leq x < 0.55$ and Group 2 with $0.55 < x \leq 1.0$. Group 1 is characterized by transitions at ≈40 K and ≈80 K, being close to those in Nb_3Te_4, whereas Group 2 by those at ≈50 K and ≈140 K. These transitions are respectively referred to as the 40-K, 80-K, 50-K, and 140-K transition. The nature of the Group 1 transitions is considered to be substantially identical with that found in binary Nb_3Te_4 due to the correspondence between the transition temperatures. The 80-K transition is therefore considered to be caused by the same type of CDW transition as observed in Nb_3Te_4. Although observations of the formation of CDWs were attempted at low temperatures for the Group 1 samples, none were found.

The mechanisms responsible for the transitions in Group 2 samples may also be similar to that found in Nb_3Te_4 because of the correlation between their temperature variations of ρ around T_t. However, the discon-

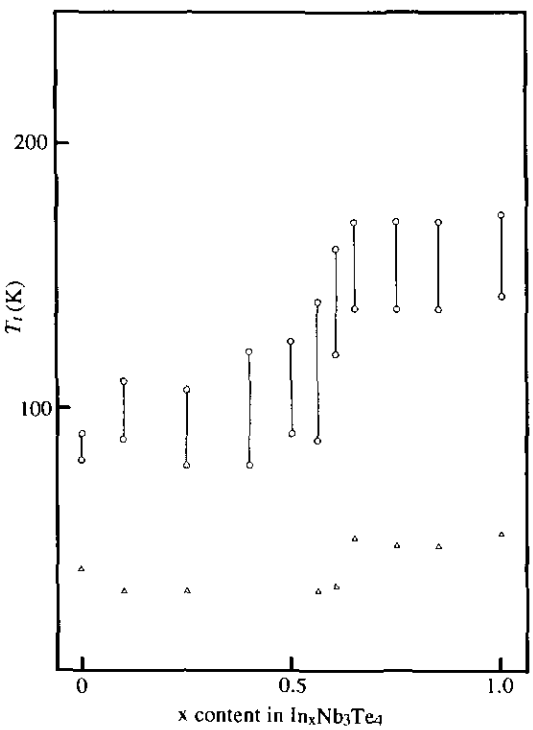

FIG. 8. Transition temperature T_t in $In_xNb_3Te_4$ as a function of In content x observed in the ρ measurements. The top and the bottom of the vertical bars respectively indicate the onset and the maximum temperature in the ρ vs T curves (Fig. 7).

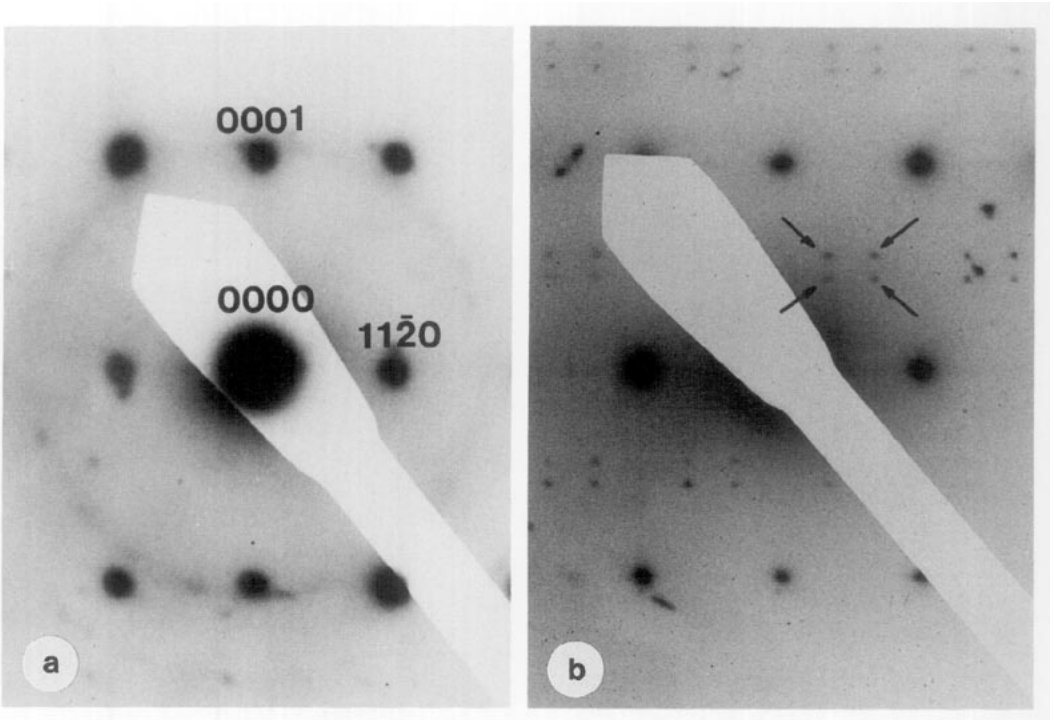

FIG. 9. Electron diffraction patterns of $In_{0.75}Nb_3Te_4$ taken at room temperature (a) and at ≈60 K (b). The incident electron beam is the direction of [1$\bar{1}$00].

tinuous change of T_t at $x \simeq 0.55$ suggests a change in the transition nature near this composition. ED observations were conducted at low temperatures to observe this phenomena, and Fig. 9a and b respectively show the ED patterns of $In_{0.75}Nb_3Te_4$ taken at room temperature and ≈60 K. The incident electron beam is the direction of [1$\bar{1}$00], being identical to that used by Suzuki *et al.* (*22*). The superlattice reflections are shown at ≈60 K, and are characterized by commensurate wave vectors $q = \pm(\frac{1}{3}a^* + \frac{1}{3}b^*) + \frac{4}{9}c^*$. As mentioned previously, Sekine *et al.* (*23*) found wave vectors of $q = \pm(\frac{1}{3}a^* + \frac{1}{3}b^*) + \frac{3}{7}c^*$ in Nb_3Te_4 below the 80-K transition using X-ray diffraction measurements, and the present results are consistent except for the slight increase in the value of c^*. Thus, it is quite likely that the 140-K transition in the Group 2 samples is due to a CDW formation which is caused by a mechanism similar to that occurring in Nb_3Te_4. Sekine *et al.* pointed out that the value of $\frac{3}{7}c^*$ is nearly equal to twice the Fermi wave vectors of the two outer Fermi surfaces ($\approx 0.25c^*$ and $\approx 0.17c^*$) calculated by Oshiyama (*16, 17*), and suggested that this situation may be favorable for the formation of the CDW state in Nb_3Te_4. This is considered reasonable because of the strong one-dimensional nature of the energy band structure in this compound (*16–19*). Using the same rationale, the increase in the c^* component of the q vectors in the present data could be explained if the Fermi level is raised slightly higher by the In insertion, possibly caused by the subsequent charge transfer from the In atoms to the Nb atoms in the host lattice. This hypothesis is quite feasible since the conduction bands in this

compound have a *d*-band character originating from the Nb–Nb chains along the *c* axis (*18*). The increase of the Fermi energy then leads to an increase in the c^* component of the Fermi wave vectors. Consequently, the c^* component in the q vectors of the CDW found here would increase in such a way as to satisfy the nesting conditions for CDW formation. Sekine *et al.* (*23*) reported that the appearance of the a^*–b^* components of the q vectors is due to an ordering of the CDW phases on the individual Nb–Nb chains, a phenomenon which originates from interactions occurring between the chains. The fact that the values of the a^*–b^* components of the q vectors in the present case are same as in Nb_3Te_4 indicates that the interaction between the Nb chains is not varied by the In insertion. The same superlattice spots were observed in $In_{0.65}Nb_3Te_4$ at ≈60 K, yet did not appear in other samples containing a greater In content x. Sekine *et al.* (*23*) suggested the 30-K transition in Nb_3Te_4 is possibly due to the formation of a CDW, and even though ED patterns were not observed below 50 K, Group 2's 50-K transition may be also associated by the formation of a CDW having a different superstructure from that of the 140-K transition. Nonlinearity of the DC resistivity ρ below the 140-K transition was not found, being compatible with the commensurate superstructures existing below the transition. In addition, nonlinearity of ρ was not observed below the 50-K transition.

Figure 10 shows the temperature dependence of the Seebeck coefficient S for polycrystalline $In_xNb_3Te_4$ samples with $x = 0$, 0.65, and 1.0. It should be noted that S reaches a maximum at ≈110 K for Nb_3Te_4, and at 150–160 K for the $x = 0.65$ and 1.0 samples. Each anomaly respectively corresponds to the phase transition observed in the ρ measurements. In all the samples, the value of S above the transition slightly decreases almost linearly with decreasing temperature. The increase in S at the anomaly

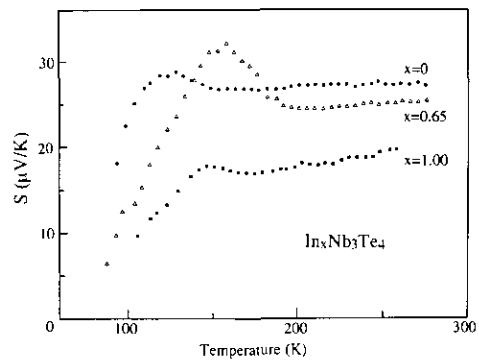

FIG. 10. Temperature variations of Seebeck coefficient S of polycrystalline $In_xNb_3Te_4$ ($x = 0$, 0.65, and 1.0).

can be explained by the semiconductive nature appearing at the transition as observed in the ρ measurements. Above the transition, S is ≈20–30 μV/K, and shows a tendency to decrease with increasing In content x. The positive values of S indicate that in this temperature range the dominant carriers are holes. In a simple uncorrelated metal without electron–phonon interactions (phonon drag), S is given by

$$S = \pi^2 k_b^2 T / e E_F, \qquad (1)$$

where k_b is the Boltzmann constant and E_F the Fermi energy. Although the extrapolated lines of the S vs T curves above T_t do not intercept the origin, the linear temperature dependence of S above T_t, as well as the relatively small values of S, suggests that these compounds have normal metallic characteristics above T_t. By applying Eq. (1) to the present results which indicate that S decreases with increasing x above T_t, we can speculate the Fermi energy is raised slightly higher with increasing x. It should be noted that this speculation is consistent with the previous discussion concerning the increase of c^* in the q vectors as observed in ED patterns of Fig. 9b. The observed hole-like conduction conflicts with the results of Ishihara *et al.* (*21, 27*) who reported

TABLE I

SUPERCONDUCTING CRITICAL TEMPERATURE T_c AND TRANSITION TEMPERATURE T_t FOR $In_xNb_3X_{4-y}$ (X = S, Se, AND Te)

	T_c (midpoint) (K)	T_t (maximum) (K)
	$In_xNb_3S_{3.84}$	
$x = 0$	3.5	—
0.25	*	—
0.50	2.1	—
	$In_xNb_3Se_{3.84}$	
$x = 0$	*	—
0.10	*	—
0.25	*	—
0.40	2.5	29
0.50	2.4	22
0.60	2.6	28
0.75	2.0	26
1.00	2.7	28
	$In_xNb_3Te_4$	
$x = 0$	*	40 80
0.10	*	36 88
0.25	*	35 78
0.40	*	— 78
0.50	*	35 90
0.55	*	30 88
0.60	*	32 120
0.65	4.4	50 138
0.75	3.0	48 137
0.88	3.3	48 138
1.00	3.0	52 142

Note. * indicates that T_c was not observed above 1.5 K.

that S is negative in the c direction of the single crystals of Nb_3Te_4 over a wide temperature range. This discrepancy may originate from the difference between the measured sample forms, i.e., polycrystals in the present study and single crystals in Ishihara *et al.*, hence suggesting these tellurides have a strong anisotropy in S, e.g., S is negative along the c axis and positive perpendicular to the c direction.

Table I summarizes resultant superconducting critical temperatures T_c (midpoint value) and transition temperatures T_t (maximum point in ρ vs T curves). T_c was not observed above 1.5 K in either $Nb_3Se_{3.84}$ or Nb_3Te_4, possibly being caused by the presence of a small deviation of chalcogen compositions from the stoichiometry. In the $In_xNb_3Se_{3.84}$ system T_c was observed from 2.0 to 2.7 K when $0.4 \leq x \leq 1.0$. On the other hand, when $x \leq 0.25$, a T_c above 1.5 K was not observed. If the phase transition at 25–45 K in this system is of a CDW-type, the coexistence of the superconductivity and the CDW state is realized in $In_xNb_3Se_{3.84}$ system as in the tellurides. Thus, the nature of the phase transition in the selenides must be revealed by other methods such as X-ray diffraction measurements. In the tellurides, $T_c > 1.5$ K was not observed when $x \leq 0.60$, yet when $x \geq 0.65$, T_c appears above 3.0 K. The increase in Group 2's T_c value may be a result of the CDWs having different characteristics than in Group 1. In conclusion, it is believed that the present compounds are excellent materials to provide a foundation from which to elucidate the correlation phenomena between the superconductivity and CDW states. Now more detailed diffraction measurements will be attempted for the further elucidation of this phenomena.

Acknowledgments

One of the authors (T. O.) thanks Messrs. M. Ohhashi, M. Sakai, and Y. Nojima for their technical assistance. The authors are grateful to Professor H. Hashimoto and Dr. K. Suzuki for their fruitful advices on the electron microscopic observations. This work was supported in part by a Grant-in-Aid for Scientific Research from the Ministry of Education.

References

1. J. A. WILSON, F. J. DISALVO, AND S. MAHAJAN, *Phys. Rev. Lett* **32,** 882 (1974); *Adv. Phys.* **24,** 117 (1975).
2. For example, G. GRÜNER AND P. MONCEAU, *in* "Charge Density Waves in Solids" (L. P. Gorkov and G. Grüner, Eds.), pp. 137, North-Holland, Amsterdam/Oxford/New York/Tokyo (1989).
3. K. SELTE AND A. KJEKSHUS, *Acta Crystallogr.* **17,** 1568 (1964).

4. A. F. Ruysink, A. Kadijk, A. J. Wagner, and F. Jellinek, *Acta Crystallogr. Sect. B* **24,** 1614 (1968).
5. M. Vlasse and L. Fournès, *Mater. Res. Bull.* **11,** 1527 (1976).
6. T. Ohtani and S. Onoue, *J. Solid State Chem.* **59,** 324 (1985).
7. H. Boller and K. Klepp, *Mater. Res. Bull.* **18,** 437 (1983).
8. T. Ohtani and S. Onoue, *Mater. Res. Bull.* **21,** 69 (1986).
9. K. D. Bronsema and G. A. Wiegers, *Mater. Res. Bull.* **22,** 1073 (1987).
10. R. Schöllhorn and W. Schramm, *Z. Naturforsch. B* **34,** 697 (1979).
11. G. Huan and M. Greenblatt, *Mater. Res. Bull.* **22,** 505 (1987).
12. G. Huan and M. Greenblatt, *Mater. Res. Bull.* **22,** 943 (1987).
13. E. Amberger, K. Polborn, P. Grimm, M. Dietrick, and B. Obst, *Solid State Commun.* **26,** 943 (1978).
14. Y. Ishihara and I. Nakada, *Solid State Commun.* **42,** 579 (1982).
15. Y. Ishihara and I. Nakada, *Solid State Commun.* **44,** 1439 (1982).
16. A. Oshiyama, *Solid State Commun.* **43,** 607 (1982).
17. A. Oshiyama, *J. Phys. Soc. Jpn.* **52,** 587 (1983).
18. D. W. Bullett, *J. Solid State Chem.* **33,** 13 (1980).
19. E. Canadell and M.-H. Whangbo, *Inorg. Chem.* **25,** 1488 (1986).
20. Y. Ishihara and I. Nakada, *Solid State Commun.* **45,** 129 (1983).
21. Y. Ishihara and I. Nakada, *Jpn. J. Appl. Phys.* **23,** 851 (1984).
22. K. Suzuki, M. Ichihara, I. Nakada, and Y. Ishihara, *Solid State Commun.* **52,** 743 (1984); **59,** 291 (1986).
23. T. Sekine, Y. Kiuchi, E. Matsuura, K. Uchinokura, and R. Yoshizaki, *Phys. Rev. B* **36,** 3153 (1987).
24. A. Briggs, P. Monceau, M. Nunez-Requeiro, J. Peyrard, M. Ribault, and J. Richard, *J. Phys. C Solid State Phys.* **13,** 2117 (1980).
25. A. Meerschaut and J. Rouxel, *in* "Crystal Chemistry and Properties of Materials with Quasi-One-Dimensional Structure" (J. Rouxel, Ed.), p. 205, Reidel, Dordrecht/Boston/Lancaster/Tokyo (1986).
26. T. Ohtani, *J. Phys. Soc. Jpn.* **37,** 701 (1974).
27. Y. Ishihara, I. Nakada, K. Suzuki, and M. Ichihara, *Solid State Commun.* **50,** 657 (1984).